AD-A086 386 AERONAUTICAL RESEARCH LABS MELBOURNE (AUSTRALIA) F/G 14/2
ULTRASONIC CAUSTICS IN NON-DESTRUCTIVE EVALUATION.(U)
JUL 79 P A DOYLE
UNCLASSIFIED ARL/MAT. 111 NL

1 OF 1
AD A086386

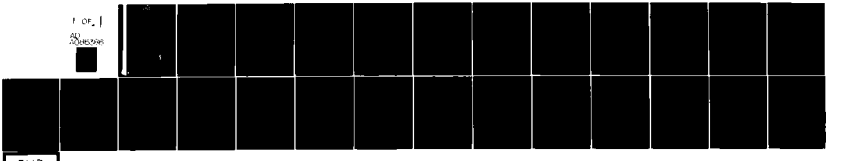

END
DATE FILMED
8-80
DTIC

ARL-MAT-REPORT-111

AR-001-747

DEPARTMENT OF DEFENCE

DEFENCE SCIENCE AND TECHNOLOGY ORGANISATION

AERONAUTICAL RESEARCH LABORATORIES

MELBOURNE, VICTORIA

MATERIALS REPORT 111

ULTRASONIC CAUSTICS IN NON-DESTRUCTIVE EVALUATION

by

P. A. DOYLE

COPY No 12

JULY, 1979

AR-001-747

DEPARTMENT OF DEFENCE
DEFENCE SCIENCE AND TECHNOLOGY ORGANISATION
AERONAUTICAL RESEARCH LABORATORIES

12

MATERIALS REPORT 111

11) Jul 77

(6)

ULTRASONIC CAUSTICS IN NON-DESTRUCTIVE EVALUATION,

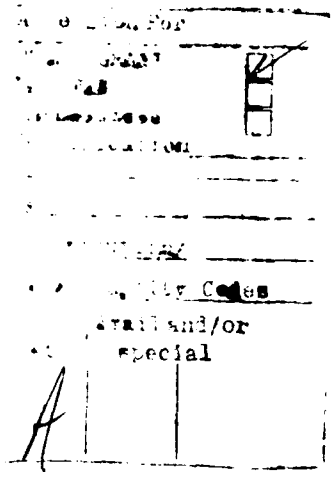

by

P. A. DOYLE

9) Technical Report

(14) ARL/MAT. 111

SUMMARY

Caustics formed in the field diffracted by defects are explored theoretically as a possible approach to the inverse scattering problem for ultrasonic non-destructive evaluation. The case of crack-like defects is considered in detail using the geometrical theory of diffraction. The involute of the far field caustic reproduces the projection of the crack edge in the incident beam direction, for a plane incident wavefront. This purely geometrical inversion is carried out uniquely for the astroid and its involute, the elliptical edge. For a general edge shape, the complete inversion requires one further length measurement, which may be carried out in some cases by further experiments with caustics. Useful limitations on the possible shapes of caustics are explained on the basis of catastrophe theory. Calculations show that the inherent intensity level change (~2–3 dB) and width (~wavelength) over which it occurs for a typical ultrasonic caustic are adequate for observation. Some discussion is given of experimental requirements, as well as of caustics formed in the near field of a crack and of those formed by voids and inclusions. The topology of the far field caustic cannot in general distinguish between volumetric and crack-like defects. Studying caustics may prove to be a useful adjunct to ultrasonic imaging systems for the inspection of fatigue cracks.

10) Peter M. / Doyle

POSTAL ADDRESS: Chief Superintendent, Aeronautical Research Laboratories,
Box 4331, P.O., Melbourne, Victoria, 3001, Australia.

DOCUMENT CONTROL DATA SHEET

Security classification of this page: Unclassified

1. Document Numbers
   (a) AR Number: AR-001-747
   (b) Document Series and Number: Materials Report 111
   (c) Report Number: ARL-Mat Report 111

2. Security Classification
   (a) Complete document: Unclassified
   (b) Title in isolation: Unclassified
   (c) Summary in isolation: Unclassified

3. Title: ULTRASONIC CAUSTICS IN NON-DESTRUCTIVE EVALUATION

4. Personal Author: Doyle, Peter A.

5. Document Date: July, 1979

6. Type of Report and Period Covered: Technical Report

7. Corporate Author(s): Aeronautical Research Laboratories

8. Reference Numbers
   (a) Task: DST 76/95
   (b) Sposoring Agency:

9. Cost Code: 34 4790

10. Imprint: Aeronautical Research Laboratories, Melbourne

11. Computer Program(s) (Title(s) and language(s)):

12. Release Limitations (of the document)
    Approved for public release

12-0. Overseas:	N.O.		P.R.	1	A		B		C		D		E	

13. Announcement Limitations (of the information on this page): No Limitation

14. Descriptors:
    Ultrasonic scattering
    Inverse scattering problem
    Nondestructive tests
    Catastrophe theory
    Geometrical diffraction theory

15. Cosati Codes:
    2001
    1402

16. *ABSTRACT*

Caustics formed in the field diffracted by defects are explored theoretically as a possible approach to the inverse scattering problem for ultrasonic non-destructive evaluation. The case of crack-like defects is considered in detail using the geometrical theory of diffraction. The involute of the far field caustic reproduces the projection of the crack edge in the incident beam direction, for a plane incident wavefront. This purely geometrical inversion is carried out uniquely for the astroid and its involute, the elliptical edge. For a general edge shape, the complete inversion requires one further length measurement, which may be carried out in some cases by further experiments with caustics. Useful limitations on the possible shapes of caustics are explained on the basis of catastrophe theory. Calculations show that the inherent intensity level change (~2–3 dB) and width (~wavelength) over which it occurs for a typical ultrasonic caustic are adequate for observation. Some discussion is given of experimental requirements, as well as of caustics formed in the near field of a crack and of those formed by voids and inclusions. The topology of the far field caustic cannot in general distinguish between volumetric and crack-like defects. Studying caustics may prove to be a useful adjunct to ultrasonic imaging systems for the inspection of fatigue cracks.

APPROXIMATELY

CONTENTS

1. INTRODUCTION

The quantitative aim of ultrasonics in non-destructive evaluation (NDE) is to measure the shape and size of internal or surface defects in materials. Ultrasonic and acousto-optical imaging methods, pulse transit-time measurements, scattering experiments including the basic pulse-echo technique, and ultrasonic spectroscopy are the principal approaches adopted to achieve this end.

Recently, attention has been given to the central theoretical problem for ultrasonic scattering, which is the inversion of scattering data (Majda 1976; Bleistein 1976; Bleistein and Cohen 1977*a*, *b*; Whalen and Mucciardi 1978; Rose 1978; Richardson 1978; Achenbach *et al.* 1978). The present paper explores the possibility of using caustics, which are the envelopes of rays diffracted by the defect, for this inversion. Caustics are well known in optics and have been observed in other fields of scattering, such as molecular collisions (see Connor 1976) and diffuse scattering of X-rays and neutrons by dislocation loops (Trinkaus 1971).

The theory below is developed for a crack-like defect of almost any shape, which need not lie in a single plane. The elliptical crack is analyzed in detail, and some comments are made concerning voids and inclusions. The simple relationship between the caustic patterns and the diffracting object (defect) is explained on the basis of the geometrical theory of diffraction (Keller 1957), and general limitations on the shapes of caustics which could assist in their identification are discussed. Section 3 gives some examples of diffracting object/caustic pairs, and describes methods for the geometrical inversion of the caustic. Section 4 calculates the inherent width and intensity level change for caustics, and considers the possibilities for experimental observation. The discussion outlines the potential value of caustics for fatigue crack imaging, and the types of caustics expected from scattering by voids and inclusions.

2. THEORY

The case of most practical importance in NDE concerns the scattering of elastic waves in a solid. It will become clear below that the geometry of caustic surfaces for elastic waves can be inferred from that of waves in the scaler wave case. For an incident plane wave, we are therefore concerned with solutions for the scattered wave amplitude u of the reduced wave equation

$$\Delta u + k^2 u = 0 \tag{1}$$

where k is the wave number. Diffraction by the edge of a two-dimensional crack-like object, which in general is not planar, will be discussed in this section. The radius of curvature at all points on the edge is assumed to be large compared with $2\pi/k$.

Asymptotic solutions of equation (1) are given by Keller's geometrical theory of diffraction (see e.g. Lewis and Beorsma 1969), in which u is assumed to be of the form

$$u \sim \exp\{i\,k\,\phi(\mathbf{y})\} \sum_{m=0}^{\infty} (ik)^{-m}\, z_m(\mathbf{y}), \quad k \to \infty \tag{2}$$

Inserting equation (2) into equation (1) gives the eikonal equation for the phase function $\phi(\mathbf{y})$ and a recursive set of transport equations for the amplitude function $z_m(\mathbf{y})$. In particular, the first and most important term $m = 0$ can be writen as

$$u \sim A\{\gamma/(\gamma + \sigma)\sigma\}^{1/2} \exp\{i\,k\,\phi(\boldsymbol{\sigma}, s)\} \tag{3}$$

where $\boldsymbol{\sigma}$ is the vector (of magnitude σ) between the field point $\mathbf{y}$ and the point $\mathbf{x}(s)$ on the edge, and s measures arc length along that edge (Fig. 1). The parameter γ is the distance from a point $\mathbf{x}$ to the other caustic along the ray (the edge itself is one caustic of the astigmatic pencil of diffracted rays). The phase function is related to the phase $\phi_0(s)$ of the incident wave at the edge

by $\phi(\sigma, s) = \phi_0(s) + \sigma$. The amplitude factor A is found in Keller's theory by comparison with the exact solution for the appropriate canonical problem, which for diffraction by a smooth edge is the half-plane result of Sommerfeld (1954). This comparison technique is central to much of the success enjoyed by the geometrical theory, though it is not important for the present paper.

In his original theory, Keller (1957) derived equation (3) by considering directly the conservation of energy along a ray tube. Clearly this approach breaks down at caustics, where $\sigma = -\gamma$, and at shadow or reflection boundaries, where A becomes infinite (Ahluwalia, Lewis and Boersma 1968). This failure results because equation (2) is an inappropriate assumption for the asymptotic form of u in these regions. In the neighbourhood of a caustic, the field should be written as a superposition of plane waves

$$u(\mathbf{y}) = \int_{\text{edge}} z(\sigma, s) \exp\{ik\phi(\sigma, s)\}\, ds \tag{4}$$

This integral around the diffracting edge is the starting point for the theory of Kravstov (1964) and Ludwig (1966), who derive expressions for u which are uniformly valid for a field containing a caustic.

For large k, the diffraction integral in equation (4) can be evaluated by the stationary phase method, which states that the dominant contributions to $u(\mathbf{y})$ come from points on the edge where the derivative $\phi_s = 0$. If β is the angle between the incident ray and the tangent $\mathbf{t}$ to the edge at s (Fig. 1), the field at $\mathbf{y}$ is due to rays which satisfy the condition

$$\phi_s(\sigma, s) = \cos\beta(s) - \boldsymbol{\sigma}\cdot\mathbf{t}/\sigma = 0 \tag{5}$$

This equation defines the well-known cones of diffracted rays of semi-angle $\beta(s)$ emanating from points on the edge, whose geometry Keller (1957) predicted simply by extending Fermat's principle, in the limit of large k, to include diffraction. The envelope of these rays, which forms the caustic surface for rays diffracted once by the edge, satisfies equation (5) and also the equation $\phi_{ss} = 0$, which corresponds to the coalescence of two stationary points along the edge. This gives, for a ray $\boldsymbol{\sigma}$ to lie on the caustic surface, the equation

$$\frac{\partial(\cos\beta)}{\partial s} - \frac{\boldsymbol{\sigma}\cdot\mathbf{n}}{\sigma\rho} + \frac{\sin^2\beta}{\sigma} = 0 \tag{6}$$

where $\mathbf{n}$ is the principal normal and ρ is the radius of curvature of the edge at s. There will also be caustics formed by rays diffracted more than once by the edge, but they will be neglected in this paper because their intensity is of lower order in k (Keller 1957), and particularly because they do not occur in the same region as the caustic of the singly diffracted rays.

In the far field, equations (5) and (6) (which describe the caustic surface) reduce to those defining the caustic surface produced by the projection of the object in the incident beam direction (Keller 1957). Denoting the parameters of this projection by the superscript i, the far field caustic is then defined by

$$\boldsymbol{\sigma}^i\cdot\mathbf{t}^i = 0 \tag{7}$$

$$\boldsymbol{\sigma}^i\cdot\mathbf{n}^i = \rho^i \tag{8}$$

Equation (8) shows that the far field caustic of singly diffracted rays contains the evolute of the projection of the edge, that is the locus of the centres of curvature of points on this projection. Equation (7) shows that the far field caustic surface is a cylinder with generators in the incident beam direction, so that, in the classical limit $k \to \infty$ for which these interpretations hold, all far field cross-sections are identical. These properties, which have been derived by Keller (1957) and observed optically by Coulson and Becknell (1922) are central to the present paper: if the geometry of the far field caustic can be observed in ultrasonics, the shape and in some cases, the size of the defect projection in the incident beam direction of a crack-like object can be derived simply by constructing the involute of the caustic. The extent to which this involution can give a unique result will be discussed in section 3. The position of this classical caustic does not change with wavelength (though section 4 below shows that its height and width do change); therefore caustics can be observed with broadband, pulsed ultrasound as well as with continuous waves.

For the elastic wave case, two families of cones of singly diffracted rays occur, the second

as a result of mode conversion (Achenbach *et al.* 1978). These families are related by Snell's law, and apart from the case of normal incidence on a planar crack, two spatially separated caustic surfaces result. For example, the diffraction of a P-wave incident at $\beta_p(s)$ on the edge yields a P-wave caustic surface whose geometry is equivalent to that described by the scalar wave theory, together with an S-wave caustic. The geometry of this S-wave caustic is identical with that predicted in scalar wave theory for rays incident at various points s on the edge at angles $\arccos\{(v_s/v_p)\cos\beta_p(s)\}$, where v_p and v_s are the respective wave speeds. When $\beta_p(s)$ is significantly different from $\pi/2$, this S-wave caustic causes no complication in far field experiments because it is well separated from the P-wave caustic. Of course, the two caustics touch for points on the edge where $\beta(s) = \pi/2$, but general properties of the caustic beometry discussed below should avoid any confusion between them. In addition, S-waves can be reduced or eliminated experimentally by, for example, using as detectors normal probes with low sensitivity to S-waves, or for pulsed ultrasound, by separation in the time domain. For these reasons, a detailed analysis of caustics in elastodynamics is not essential for the present work.

Any theoretical limitations that can be placed on the possible shapes of the caustics would greatly assist their identification. For this purpose, we make use of the application of the catastrophe theory* of Thom (1975) to wave phenomena (Berry 1976). This theory is concerned with the typical local geometry of functions, in the present case those describing the caustic pattern. In the far field, this pattern depends on two co-ordinates (those of the diffracted field at infinity), as well as on the shape and size of the diffracting edge. While the *global* description of this edge requires two parameters, only one—the projected edge parameter s^t—is needed for its *local* description. The other parameter (say a polar angle) will influence the global topology of the caustic surface, but will determine only the orientation of local singularities, not their form or type. In the language of catastrophe theory, the caustic pattern then depends on just one internal parameter, so the rank is one and only cuspoid catastrophes can occur. Also, the two dimensions of the far field imply that the co-dimension of the caustic pattern in that region is two, so that only the fold catastrophe, which appears as ordinary points on the caustic surface, and cusps, are generically ('typically') possible. Since in addition 'open-ended' folds are not permitted, any normal section through the far field caustic surface produced by scattering from a purely convex edge projection typically consists of a continuous closed line interrupted only by cusps.

Non-generic caustics, which may be structurally unstable sections of higher catastrophes, can occur as a result of symmetry or by accident. However, with few exceptions such as the field scattered by a spherical void, they are unlikely to be important for the ultimate objective of ultrasonic NDE of studying real defects in solids. Berry (1976) has given some discussion of these non-generic cases, which are perhaps more easily pictured for catastrophes of rank two. Complications arise if the edge projection contains points of inflection, since the caustic then extends laterally to infinity, and appears discontinuous. These caustics would not be observed in full, so the discussion of this section excludes edge projections with concave parts; one example will be considered in section 3.

Cusps correspond to the coalescence of three geometrical ray paths, or three stationary phase points on the projection of the edge, which occurs when $\phi_s{}^t{}_s{}^t{}_s{}^t = 0$. Differentiating equation (8), this gives

$$\boldsymbol{\sigma}^t \cdot \mathbf{n}_s{}^t - \mathbf{x}_s{}^t \cdot \mathbf{n}^t = \rho_s{}^t \tag{9}$$

Using the Frenet formulae (e.g. Mathews and Walker 1964), $\mathbf{x}_s{}^t = \mathbf{t}^t$ and $\mathbf{n}_s{}^t = -\mathbf{t}^t/\rho^t$, the latter equation resulting because the projection of the edge is planar by definition, so its torsion is zero. Combining these results with equations (7) and (9), it follows that $\rho_s{}^t = 0$ for cusps in the far field caustic, i.e. cusps occur when the curvature or radius of curvature of the corresponding point on the projected edge is extremal, as is generally true for the evolutes of plane curves (e.g. Courant and John 1965). Also, the cusp is normal to the tangent at this corresponding extremal point. The importance of these properties of cusps for the geometrical inversion of scattered fields will be discussed in section 3.

In the near field of the object, we must return to equations (5) and (6) for the description of the caustic surface. Cusp lines satisfy in addition the equation $\phi_{sss} = 0$; calculating this from equation (6), no simple correlation results between cusps and distinctive geometrical features

* A useful introduction to this theory is given by Poston and Stewart (1976).

of the object, as occurs for the far field. For this reason, the far field appears more useful for simple inversion. An exception to this is the case of normal incidence on a planar object, for which the edge is trivially equivalent to its projection and the cross-section of the caustic surface is the same at any distance from the object. Unfortunately, it appears from the discussion in section 4 below that the caustic will be more difficult to observe experimentally in the far field than in the near field. Note that a near field experiment involves an additional dimension in comparison to the far field, so that the co-dimension in this case is three. Therefore the next cuspoid catastrophe can occur at those singular points along the cusp lines which satisfy $\phi_{sss} = 0$. Clear examples of these so-called 'swallowtail' catastrophes have been observed in the optical case (Berry 1976)*; however, experimental limitations discussed in section 4 may render difficult the observation in ultrasonics of the compressed form of their near singular sections.

3. RECONSTRUCTION OF THE DIFFRACTING OBJECT

The caustic pattern is always centred in the geometrical shadow of the defect, and often lies completely within this shadow. Consider firstly a diffracting edge whose projection is an ellipse with principal axes of length $2a$ and $2b$. Then the cross-section of the far field caustic will be the evolute shown in Figure 2, which is an astroid (e.g. Courant and John 1965). *Conversely*, when the caustic is observed to be an astroid, it is immediately known that the edge projection is elliptical. If the distances between the two pairs of opposite cusps are measured as $2\xi_0$ and $2\eta_0$, it follows from the equation of the astroid $(a\xi)^{2/3} + (b\eta)^{2/3} = (a^2 - b^2)^{2/3}$ that the major axis of the ellipse is $2a = -2\xi_0\eta_0^2/(\xi_0^2 - \eta_0^2)$, and $b/a = \xi_0/\eta_0$. Since the cusps are normal to the tangents at the corresponding extremal points on the edge, the ellipse is oriented as shown in Figure 2 with its major axis parallel to the line $2\xi_0$ between the closer pair of cusps. Thus it is actually not necessary to observe the complete caustic in this simple case—only the positions of cusps in the rectangular array are required.

It is useful to construct the involute of the astroid in another way, based on the knowledge that the caustic is the locus of centres of curvature of the edge. Imagine a string set along the inside of the section C_1C_2 of the astroid (Fig. 2) and extending beyond C_2 in the direction of the cusp by a distance equal to the minimum radius of curvature of the ellipse, which is known from the caustic to be $b^2/a = \xi_0^3/(\eta_0^2 - \xi_0^2)$. Unwinding this string traces out the first quadrant of the ellipse. Next, wind the string onto the section C_1C_4 of the astroid to produce the second quadrant of the ellipse. Proceeding clockwise around the astroid and alternately winding and unwinding in this way, the complete ellipse is generated in an anticlockwise sense. This procedure also demonstrates that the arc length of the caustic between neighbouring cusps is the difference in the corresponding extremal radii of curvature.

Some special cases of the ellipse are of interest. For eccentricity $\epsilon \to 1$, $\xi_0 \to a$ so that $\eta_0 \to \infty$, i.e. one pair of cusps extends laterally to infinity and is not observed. Therefore, tilting the object about the axis of the closer pair of cusps enables direct measurement of the major axis, since the two remaining cusps become coincident with the ends of the narrow shadow boundary. Also, for $\epsilon \to 0$, the edge approaches a circle and $\xi_0 \simeq \eta_0 \to 0$. Therefore, for ellipses of low eccentricity, the four cusps form an approximately square array which will be too small to resolve. Ultimately, for the circle $\epsilon = 0$ and the cross-section of the caustic pattern degenerates to a single point, which is well known in optics to have an intensity equal to that of the incident field (e.g. Born and Wolf 1959). Observation of such a degenerate caustic immediately gives the projection of the diffracting edge as being circular. This particular case is not described in the classification given by Thom's theorem because of its high symmetry. The size of a nearly circular defect may be found by tilting the specimen, giving an elliptical projection whose caustic is an astroid of convenient dimensions.

Some other examples of caustic/diffracting edge pairs can be generated from the elliptical case. If one side of a distorted ellipse is flatter than the other, a caustic will result which has two pairs of cusps arrayed at right angles, but not symmetrically (Fig. 3*a*). Again, if an ellipse is distorted by shifting one turning point from the symmetrical position, the cusps will no longer

* The author is indebted to Dr. M. V. Berry for private communication on this point, and for reading the manuscript.

be directed as two opposing pairs at right angles (Fig. 3*b*). Nevertheless, the directions of the tangents at the turning points are immediately known by inspection of the caustic.

If the edge projection contains a concave part, the caustic will appear discontinuous, since it extends to infinity at points of inflection. Figure 4 shows an ellipse 'pressed in' at one end, and the corresponding caustic. Note that the intensity of the caustic tends to zero far out along those sections which are asymptotic to the normal at the points of inflection, because the density of contributing ray paths then approaches zero. Therefore, only a limited part of the caustic will actually be observed. A less severe depression in the end of the ellipse will produce the cusp marked *D* further away from the rest of the caustic. A 'flattened end' on an ellipse which is nevertheless convex will give a caustic section as a closed line containing six cusps. Three of these cusps coalesce into one as the distortion of the ellipse is reduced to zero, again producing the simple 4-cusped astroid.

Involuting the far field caustic gives the projection of the diffracting edge in the incident beam direction. The orientation of a planar defect in three dimensions could be inferred from several such measurements involving different projections. Another approach is to examine the variation of the caustic pattern as the plane of observation is moved into the near field: the special case of normal incidence produces no change of the caustic in this region. Identifying this behaviour defines the normal to a planar defect. The extent to which the three dimensional structure of non-coplanar diffracting edges can be found is not considered here, both because of its greater complexity and because most practical applications of defect sizing in ultrasonics do not require this detail.

Any smooth, purely convex closed shape has an even number of turning points, since maxima and minima of curvature must alternate in circuit. Therefore, there is an even number of cusps in the caustic which is itself a partial check on an experiment. The diffracting edge projection is normal to the cusps at the points of extremal curvature, so the orientation of the projection is known by inspection of the cusps. Edge projections corresponding to caustics of four, six, eight or higher even number of cusps can be constructed by alternately folding and unfolding each caustic section in turn, just as was done for the ellipse. For this general case, there is no representation of the caustic in terms of elementary functions as there was for the astroid. Therefore, the radius of curvature at one extremal point cannot be deduced simply from the spacing of cusps, and a different method must be sought to achieve a unique reconstruction.

Since the cusps corresponding to the minima of $\rho(s)$ are less sharp than those corresponding to maxima (e.g. see the ellipse of Fig. 2), it should be possible to identify at least one cusp corresponding to a minimum of $\rho(s)$, say ρ_1. Beginning with this cusp, and assuming particular values for ρ_1, a one-parameter family of possible involutes of the caustic can be generated. It then remains to choose the correct involute from this set. One technique suitable for some cases of planar defects would be to tilt the object about an axis between two approximately opposite cusps, whose spacing would then be asymptotic to the length of the narrow shadow boundary. This procedure enables direct measurement of one length in the diffracting edge, which is sufficient to select the correct involute. If one length in the edge can be determined by a different technique, as is possible for some objects using ultrasonic spectroscopy (e.g. Bifulco and Sachse 1975, Adler *et al.* 1977), the desired involute can again be chosen from the set of possibilities.

Trinkaus and Drepper (1977) show for the more general case of a two dimensional phase object how to derive the curvatures of extremal points from the positions and intensities of the peaks in the diffracted field which 'clothes' the caustic in the neighbourhood of the cusps. However, it can be shown that the transitional approximation which they use to calculate the relevant diffraction integral is not accurate sufficiently far from the position of the classical caustic for typical ultrasonic values of k, which are of course much smaller than those for optics. Therefore, adapting their method to ultrasonics would require the more accurate uniform approximation for the diffraction integral (e.g. Felsen and Marcuvitz 1973); the resulting procedure would be too complicated to be attractive for ultrasonic NDE. In any case, the spacing of the 'Airy fringes' in ultrasonics is near the resolution limit of imaging systems, as discussed in section 4 below. The work of Trinkaus and Drepper nevertheless does suggest that a unique inversion is possible for more general edge shapes.

Further work pursuing the selection of a unique inversion may be profitable, for instance by developing formulae for special geometries as was done for the astroid and its involute.

At present, however, it is important to ask how difficult it will be to locate caustics in ultrasonics. This question is addressed in the following section.

4. CALCULATED CONTRAST AT THE CAUSTIC AND ITS POSSIBLE OBSERVATION

The ease of observation of caustics in ultrasonics will depend on their width as well as their intensity relative to the background in their neighbourhood. These properties will be studied by considering a particular but typical case, specifically normal incidence of a plane wavefront on a planar elliptical crack, described parametrically by $x = a\cos\theta$, $y = b\sin\theta$. Calculations will be made for a point on the caustic which lies within the geometrical shadow of the ellipse; the contrast will be low for any part of the caustic which lies outside this shadow in the bright field of the incident wave.

Referring again to Figure 2, we see that the coalescence of two stationary phase points at $\theta = \pi/4$, for example, contributes to the caustic surface along a line which projects into the astroid segment C_1C_2 at point P. In addition, these rays from $\theta = \pi/4$ contribute as from an isolated stationary point to caustic segments in the first and third quadrants, respectively before and after passing through the caustic. Equivalently, there are two 'isolated' contributions from the fourth and second quadrants to the field at all points along the caustic line through P. The question then reduces to a comparison between the intensity on the 'bright side' of the caustic (the inside of the astroid), to which four rays contribute including two which coalesce, and the intensity on the 'dark side' to which two rays contribute.

For the planar crack specified, the function $z(\sigma, s)$ in the diffraction integral (equation 4) is proportional to σ^{-1}. If the constant of proportionality, which depends on the amplitude of the incident wave, is set equal to unity, the intensity u_I^2 scattered to a point $\mathbf{y}$ in the far field from an isolated stationary point s_I is (adapting e.g. Skudrzyk 1971)

$$u_I^2(\mathbf{y}) = 2\pi\{k\sigma^2\phi_{ss}(s_I)\}^{-1} \tag{10}$$

For two stationary points coalescing at s_C, $\phi_{ss} \to 0$ and equation (10) should be replaced by the transitional approximation

$$u_C^2(\mathbf{y}) = \frac{4\pi^2}{\sigma^2}\left\{\frac{2}{k\phi_{sss}(s_C)}\right\}^{2/3} Ai^2(-\delta) \tag{11}$$

where the argument of the Airy integral is given near the caustic (Ludwig 1966) by

$$\delta = \{2k^2/|\alpha|\}^{1/3} d \tag{12}$$

In equation (12), α is the radius of curvature of the *caustic* and d is the perpendicular distance from the field point $\mathbf{y}$ to the caustic. Recalling that $\phi(s) = \phi_0(s) + \sigma$, and making use of the ray condition (equation 5) for $\beta(s) = \pi/2$, the remaining functions in equations (10) and (11) are found to be

$$\phi_{ss}(s_I) = \{1 - \boldsymbol{\sigma}\cdot\mathbf{n}/\rho\}/\sigma \tag{13}$$

$$\phi_{sss}(s_C) = \rho_s/(\sigma\rho) \tag{14}$$

For the far field, σ can now be replaced by the distance z_0 between the diffracting object and the plane of observation of the caustic section.

The intensity on the dark side of the caustic is found by summing incoherently the contributions from the appropriate isolated edge points, s_1 and s_2. This procedure ignores any interference between these two rays; any resulting intensity variation would in any case be smoothed by an experiment using a broadband transducer. On the bright side of the caustic, the maximum intensity is the sum of these two rays plus the maximum value of the caustic field, which occurs at $\delta = 1{\cdot}02$. The parameters ρ and ρ_s for the edge, α for the caustic and $\boldsymbol{\sigma}\cdot\mathbf{n}$ for the edge points s_1 and s_2 are found in Appendix I for the elliptical crack for $\theta = \pi/4$ and its corresponding caustic along the line through P. Table I lists the maximum contrast

$$C_{max} = \frac{u^2_{Cmax} + (u_1^2 + u_2^2)}{(u_1^2 + u_2^2)}$$

at the caustic section 100 mm behind the plane of the ellipse $(a, b) = (10, 7{\cdot}5)$ mm for 10 MHz

in water and typical P and S wavelengths in steel. The calculated changes in intensity level of the order of 3·5–5 dB can easily be observed experimentally. In addition, Table I gives estimates of the contrast C_{av} predicted if $Ai^2(-\delta)$ is averaged over its first two fringes; the changes of intensity level of about 2–3 dB are also observable.

Examination of equations (10)–(14) shows that the intensity contributed by isolated edge points decreases as σ^{-1} for large σ, which is expected since each point on the edge scatters as an infinitesimal section of an infinite half-plane, which gives a cylindrical wave. The caustic intensity decreases more rapidly, as $\sigma^{-4/3}$. The contrast at the far field caustic therefore decreases weakly as $\sigma^{-1/3}$, so the choice for σ (that is, z_0) is not critical from this theoretical viewpoint. Practical limitations of transducers are more important for choosing z_0, as discussed below. Equations (10) and (11) also show that the values for C increase only as $k^{1/3}$, so a reasonable estimate of C in an experiment is found by taking k to correspond to the centre frequency of the transducer; it is not necessary to integrate over the spectrum, though this could readily be done.

An estimate of the width of the caustic is the distance d_W from the maximum intensity on the bright side to the position on the dark side where u_C^2 has dropped to 10% of its maximum value. Equations (11) and (12) then give

$$d_W = 1{\cdot}8\{\alpha/2k^2\}^{1/3} \tag{15}$$

The values of d_W in Table I are of the order of the corresponding wavelength λ, or slightly greater. Since λ is also a rough estimate of the resolution that can be achieved in any scanning or imaging system which may be used to measure the field, it is clear that the inherent width of the contrast due to caustics should not prevent their observation. This conclusion becomes less valid as α increases, such as for the part of the caustic corresponding to edge points near the minor axis of a highly eccentric ellipse. Therefore for the technique proposed in section 3 which relies on tilting a plane crack about an axis between two cusps, the remainder of the caustic will not only become more widespread and of lower intensity, but also more diffuse. However, since values of α for points near the two cusps become smaller on rotation, the required part of the caustic actually becomes sharper.

The spacing of the Airy fringes in ultrasonics, given at least roughly by equations similar to equation (15), are of the order of the wavelength, so these fringes will not readily be observed. This is part of the reason why caustics have been ignored in ultrasonics, whereas in the optical case $\alpha \gg \lambda$ so the fringe spacings are also much greater than λ, allowing easy observation.

Thus far, this paper has assumed a plane incident wavefront. If this wavefront is curved, as for example from a point source, the interpretation of the caustic is more complicated because its geometry depends on the curvature of the incident wave as well as on that of the edge. Nevertheless, the caustic is just as sharp and easily detected. The most important factor experimentally is to tailor the incident wave to minimize the angular spread of wavelets incident on a single point on the edge, since this spread smears out the caustic. This smearing is likely to remove any remnants of the Airy fringes, so the values for C_{av} in Table I give a more realistic estimate of the expected caustic contrast than those for C_{max}.

One approach to forming the incident field would be to use a focused ultrasonic probe, with its minimum spot set at the back focal plane of an acoustical lens to produce the convenient (though not essential) plane wavefront. Alternatively, the minimum spot could be produced by a normal probe together with another acoustical lens, which in practice can reduce the width of the generated sound to the order of λ (Knollman *et al.* 1978). Other approaches may be to exploit either the direct production of a plane wavefront from a piezoelectric plate (Lakestani *et al.* 1976), or the low divergence of beams of Gaussian cross-section (Martin and Breazeale 1971). Ultrasonic point sources of diameter 10 μm or less have been generated using lasers (Mallozzi *et al.* 1977), and, at the expense of complexity, these sources appear most promising for observing ultrasonic caustics. Simple geometry shows that the lateral smearing of the caustic increases with z_0, so an initial demonstration of ultrasonic caustics would most easily be carried out in the near field; in any case, the geometry of the near field caustic is identical with that of the far field for normal incidence on planar objects (section 2 above). For the actual observation of the diffracted field, any scanning or imaging system with sufficient resolution could be used. One possibility is a Schlieren system (e.g. Baborovsky *et al.* 1973); another is Bragg diffraction imaging (Korpel 1968) adapted by a suitable choice of optical lenses to image in the region behind

the object. The direct observation of a sound field by its nucleation of photographic film development in a tank of developer (Dehn 1960) may also warrant consideration.

A reasonable estimate of the width of the intensity level jump at the caustic is given by equation (15) with k corresponding to the centre frequency of the transducer. Frequency analysis is of course possible, but it is not necessary in order to observe caustics. Since d_W decreases as $k^{-2/3}$, higher frequencies (say 10–20 MHz for ultrasonic NDE) produce sharper caustics. Therefore those produced at frequencies (up to $\sim$ 2 GHz) typical of acoustical microscopes are narrow, though it must be remembered that the object under examination is small as well. Also, most microscope systems are not designed to scan the diffracted field behind the object, though that based on Bragg diffraction imaging may be suitable for modification (see Korpel (1974) for a review of ultrasonic microscopy). For larger objects with correspondingly larger values of x, equation (15) shows that the caustic is only slightly more smeared out, since $d_W \propto x^{1/3}$.

5. DISCUSSION

The caustic pattern is found in and near the geometrical shadow, and its dimensions are typically comparable to those of the defect. Therefore the study of these patterns is not seen as a means of improving the resolution of imaging systems. The advantage may come in dealing with defects which, though sufficiently large, produce images that cannot be easily interpreted. For example, an image of a fatigue crack can be complicated by specular reflection from facets on the crack faces and by penetration through regions of crack closure.

To speculate further on fatigue crack imaging, first note that even for a high NDE ultrasonic intensity of 100 kWm^{-2}, the actual displacement amplitude is only about 10 Å for 10 MHz P waves in steel. Recent fracture studies by Bowles (1978) on Al alloys show that the crack tip is generally elliptical and open by several μm. Therefore for these cases the edge of the crack is opaque to ultrasound*, so the caustic can be formed by the edge. For an unloaded crack, typically less than 20% of the faces are actually closed; therefore 'false' edges inside the crack are much smaller, so their caustics will also be much smaller and either unresolved or else easily distinguished from the caustic from the 'true' edge.

In the near field of the rays transmitted by a solid or liquid filled inclusion, caustic sections described as elliptic or hyperbolic umbilics are expected, though likely to be masked by diffraction effects and experimental smearing. These catastrophes of rank two are possible because two parameters are needed for the *local* description of the defect, compared with one parameter (s) for the crack. In the far field, the co-dimension is two and again only elementary folds and cusps are generically possible. Therefore the topology of far field caustics cannot distinguish between inclusions and planar defects. This result does not hold if the orientation of the specimen is regarded as an additional accessible control parameter in the sense discussed by Berry (1976); then, singular umbilic sections can in principle be generated in the far field by rotating the specimen. Nye (1978) has carried out a detailed study of caustics of rank two for an analogous case of light passing through water droplet lenses.

For voids, umbilic sections are possible in the near field, because the local description of the source of bulk waves produced by decay of the creeping waves requires two parameters (such as s plus arc length along the geodesic). However, just as for the scattering by inclusions, these umbilics are not likely to be readily observable. The far field again consists only of elementary folds and cusps. An important singular case is the spherical void, which gives a point caustic at the centre of its shadow for all orientations. This case is not described by Thom's theorem because of its high symmetry.

The principal conclusions of this paper are:

(1) The cross-section of the ultrasonic caustic surface formed in the far field diffracted by cracks consists of a closed line interrupted only by cusps.

(2) The involute of the far field caustic section reproduces the crack edge.

(3) The geometrical inversion of the caustic can be carried out uniquely for the case of the astroid and its involute, the ellipse. For a general edge shape, the inversion gives the shape and orientation of the crack projection in the incident beam direction. A unique solution then requires one length measurement, which may be carried out in some cases by further experiments with caustics or by other means.

(4) The calculated inherent intensity level change ($\sim$2–3 dB) and width ($\sim\lambda$) over which it occurs for a typical ultrasonic caustic are adequate for observation.
(5) Experimental observation will require careful tailoring of the incident wave. Caustics may be more easily observed in the near field, though the far field is needed for simple geometrical inversion for other than normal incidence on planar defects.
(6) The study of caustics could prove to be a useful adjunct to ultrasonic scanning and imaging systems for the inspection of fatigue cracks.
(7) The topological form of far field caustics cannot in general distinguish between volumetric and planar defects. The theoretical possibility for this distinction using the near field caustic may not be experimentally viable.

* This is presumably the reason why sizing of tight fatigue cracks based on the timing of bulk wave pulses diffracted from the edge is successful, whereas the use of surface waves, which must travel over the entire crack face, breaks down (Lidington *et al.*, 1976).

APPENDIX I

Parameters for the Case of the Ellipse

For the ellipse $x = a\cos\theta$, $y = b\sin\theta$, the radius of curvature is

$$\rho = \frac{1}{ab}(a^2\sin^2\theta + b^2\cos^2\theta)^{3/2} \tag{A1.1}$$

Using $\partial s/\partial\theta = (a^2\sin^2\theta + b^2\cos^2\theta)^{1/2}$, it follows that

$$\rho_s = \frac{3(a^2 - b^2)\sin 2\theta}{2ab} \tag{A1.2}$$

The astroid is the locus of centres of curvature of the ellipse, and is given parametrically by

$$\xi = \frac{(a^2 - b^2)\cos^3\theta}{a}\,; \quad \eta = \frac{-(a^2 - b^2)\sin^3\theta}{b} \tag{A1.3}$$

The point P corresponding to rays coalescing at $\theta = \pi/4$ is

$$(\xi_p, \eta_p) = \left\{\frac{(a^2 - b^2)}{2\sqrt{2}a}, -\frac{(a^2 - b^2)}{2\sqrt{2}b}\right\}.$$

We now require the other two normals to the ellipse which pass through P. These rays occur when θ satisfies

$$-(\xi_p - a\cos\theta)\,a\sin\theta + (\eta_p - b\sin\theta)\,b\cos\theta = 0 \tag{A1.4}$$

Equation (A1.4) simplifies to

$$\sin\theta + \cos\theta = 2\sqrt{2}\sin\theta\cos\theta \tag{A1.5}$$

Equation (A1.5) can be solved by squaring both sides, then selecting the appropriate solutions for θ. The result is that the isolated stationary point contributions originate in this case at s_1 and s_2 corresponding to $\theta = 11\pi/12$ and $19\pi/12$, respectively. The function $\boldsymbol{\sigma}\cdot\mathbf{n}$ appearing in equation (13) is simply the length of the lines from s_1 and s_2 to P. For the ellipse (10, 7·5) mm, these lengths are 11·90 and 5·29 mm.

From equation (A1.3), the radius of curvature of the astroid is found to be

$$\alpha = -3ab(a^2 - b^2)\sin\theta\cos\theta\left\{\frac{\sin^2\theta}{a^2} + \frac{\cos^2\theta}{b^2}\right\}^{3/2} \tag{A1.6}$$

which is −8·08 mm at the point P for the case considered.

REFERENCES

1. Achenbach, J. D., Gautesen, A. K. and McMaken, H. 1978—In 'Elastic Waves and Non-destructive Testing of Materials' AMD Vol. 29 (Ed. YH Pao), 33–52.
2. Adler, L., Cook, K. V., Whaley, H. L. and McClung, R. W. 1977—Materials Evaluation **35**, 44–50.
3. Ahluwalia, D. S., Lewis R. M. and Boersma, J. 1968—SIAM J. Appl. Math. **16**, 783–807.
4. Baborovsky, V. M., Marsh, D. M. and Slater, E. A. 1973—Non-destructive Testing **6**, 200–7.
5. Berry, M. V. 1976—Adv. in Physics **25**, 1–26.
6. Bifulco, F. and Sachse, W. 1975—Ultrasonics **13**, 113–6.
7. Bleistein, N. 1976—J. Acoust. Soc. Am. **59**, 1259–64.
8. Bleistein, N. and Cohen, J. K. 1977*a*—J. Math. Phys. **18**, 194–201.
   1977*b*—Denver Univ. Colorado Dept. of Mathematics Report AD-A052, 908.
9. Born, M. and Wolf, E. 1959—Principles of Optics (Pergamon Press).
10. Bowles, C. Q. 1978—Delft Univ. of Technology Dept. of Aerospace Engineering Report, LR-270.
11. Connor, J. N. L. 1976—Molec. Phys. **31**, 33–5.
12. Coulson, J. and Becknell, G. G. 1922—Phys. Rev. **20**, 594–600 and 607–12.
13. Courant, R. and John, F. 1965—Introduction to Calculus and Analysis, Vol. I (Wiley).
14. Dehn, J. T. 1960—J. Acoust. Soc. Am. **32**, 1692–6.
15. Felsen, L. B. and Marcuvitz, N. 1973—Radiation and Scattering of Waves Section 4.5. (Prentice-Hall.)
16. Keller, J. B. 1957—J. Appl. Phys. **28**, 426–44.
17. Knollmann, G. C., Carver, D. and Hartog, J. J. 1978—Materials Evaluation **36**, 41–7.
18. Korpel, A. 1968—IEEE Trans Sonics and Ultrasonics *SU*-**15**, 153–7.
19. Korpel, A. 1974—In 'Ultrasonic Imaging and Holography' ed. Stroke G. W., Koch W. E., Kikuchi, Y. and Tsujiuchi, J. 345–62. (Plenum Press.)
20. Kravstov, Yu, A. 1964—Radiofizika 7, 664–73.
21. Lakestani, F., Baboux, J. C., Fleischmann, P. and Perdrix, M. 1976—J. Phys. D:Appl. Phys. **9**, 547–54.
22. Lewis, R. M. and Boersma, J. 1969—J. Math. Phys. **10**, 2291–305.
23. Lidington, B. H., Silk, M. G., Montgomery, P. and Hammond, G. 1976—Brit. J. Non-destructive Testing **18**, 165–70.
24. Ludwig, D. 1966—Comm. Pure and Appl. Maths **19**, 215–50.
25. Majda, A. 1976—Comm. Pure and Appl. Maths **29**, 261–91.
26. Mallozzi, P. J., Fairand, B. P. and Golis, M. J. 1977—In 'Research Techniques in Non-destructive Testing' Vol. 3, ed. Sharpe, R. S. 481–93. (Academic Press.)

27. Martin, F. D. and Breazeale, M. A. 1971—J. Acoust. Soc. Am. **49**, 1668–9.

28. Mathews, J. and Walker, R. L. 1964—Mathematical Methods of Physics 380–2. (New York Amsterdam: Benjamin.)

39. Nye, J. F. 1978—Proc. Roy. Soc. Lond. **A361**, 21–41.

30. Poston, T. and Stewart, I. N. 1976—Taylor Expansions and Catastrophes. (Pitman.)

31. Richardson, J. M. 1978—ARPA/AFML Review of Progress in Quantitative NDE, AFML-TR-78-205, 332–40.

32. Rose, J. H., and Krumhansl, J. A. 1978—ARPA/AFML Review of Progress in Quantitative NDE, AFML-TR-78-205, 368–73.

33. Skudrzyk, E., 1971—The Foundations of Acoustics Section 24.8 (Springer-Verlag.)

34. Sommerfeld, A. J. W. 1954—Optics. (Academic Press New York.)

35. Thom, R. 1975—Structural Stability and Morphogenesis. (Reading Mass: Benjamin.)

36. Trinkaus 1971—Z. Agnew. Phys. **31**, 229–35.

37. Trinkaus, H. and Drepper, F. 1977—J. Phys. A: Math. Gen. **10**, L11-6.

38. Whalen, M. F. and Mucciardi, A. N. 1978—ARPA/AFML Review of Progress in Quantitative NDE, AFML-TR-78-205, 341–67.

TABLE 1

Intensity changes across the caustic at point P expressed as a ratio and in dB, and caustic width, listed at 10 MHz for the section 100 mm behind an elliptical crack having semi-major axes (a, b) = (10,7·5) mm.

	Water	Steel (S)	Steel (P)
λ (mm)	0·15	0·30	0·60
C_{max}	3·12	2·68	2·32
(dB)	(4·94)	(4·28)	(3·65)
C_{av}	2·02	1·79	1·64
(dB)	(3·04)	(2·56)	(2·14)
d_W (mm)	0·24	0·37	0·60

Figure 1—The cone of rays diffracted from the incident ray at the point $\mathbf{x}(s)$ on the edge, and the geometrical definition of parameters used.

Figure 2—An elliptical diffracting edge and the corresponding far field caustic. This and figures 3 and 4 are superpositions of the spaces of the edge projection and of the far field diffraction pattern drawn on the same scale. The two cusps lying along the major axis are always inside the geometrical shadow; the other two cusps are outside the shadow for ellipses having eccentricity $>1/\sqrt{2}$. The dashed lines indicate all rays contributing to the field at point P, as discussed in section 4.

Figure 3—Distorted ellipses with their corresponding caustics.
(*a*) One side of the ellipse more eccentric than the other.
(*b*) One minimum of curvature shifted from the symmetrical position.

Figure 4—An ellipse "pressed in" at one end, and its corresponding caustic. The association between cusps and turning points is indicated by letters. The pattern in the region marked X is a superposition of elementary fold catastrophes, and should not be mistaken for a section of some higher catastrophe.

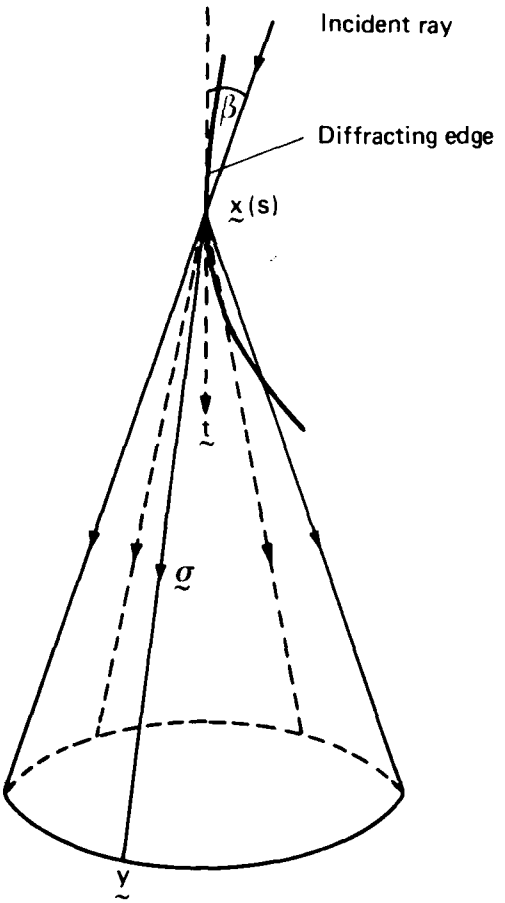

FIG. 1

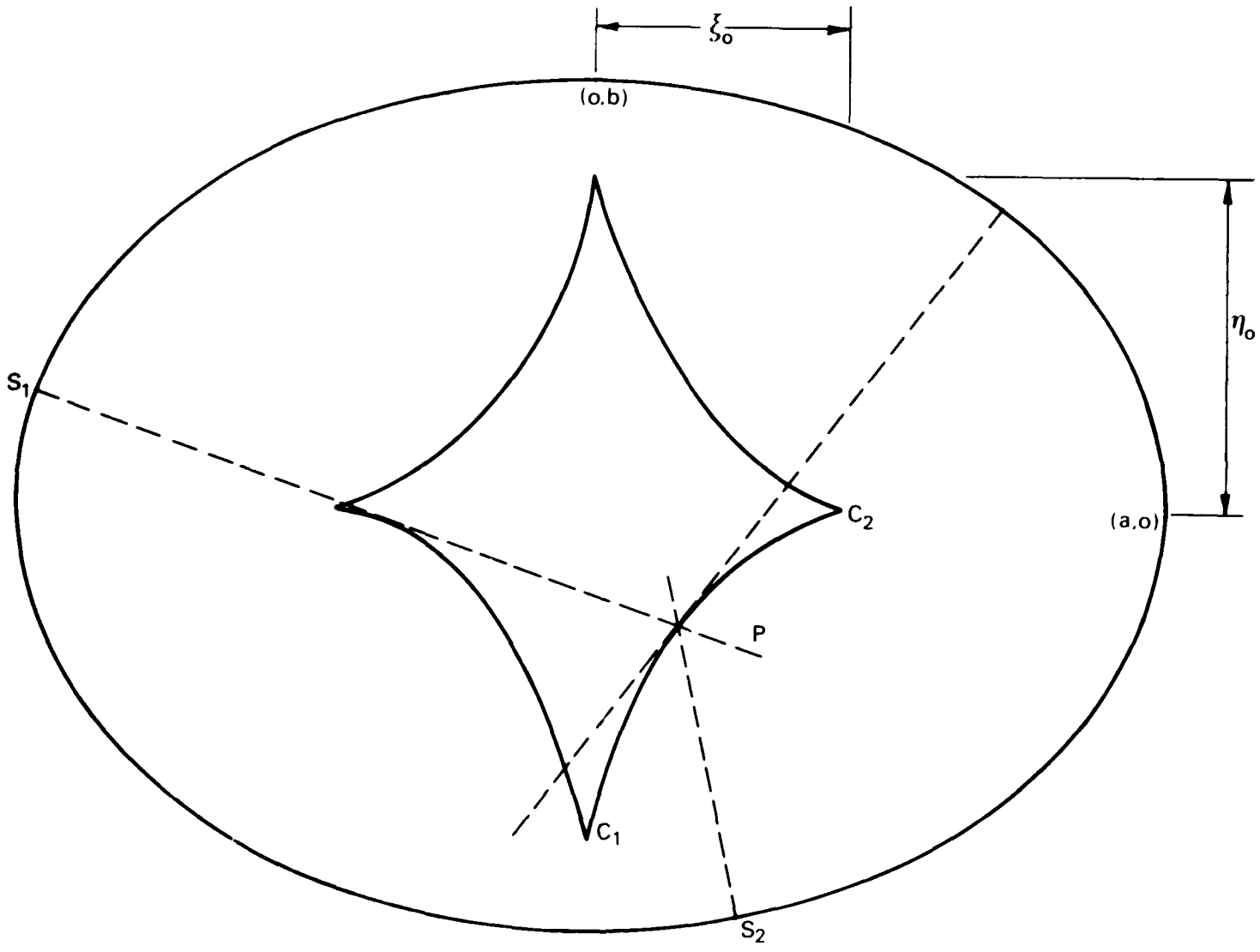

FIG. 2

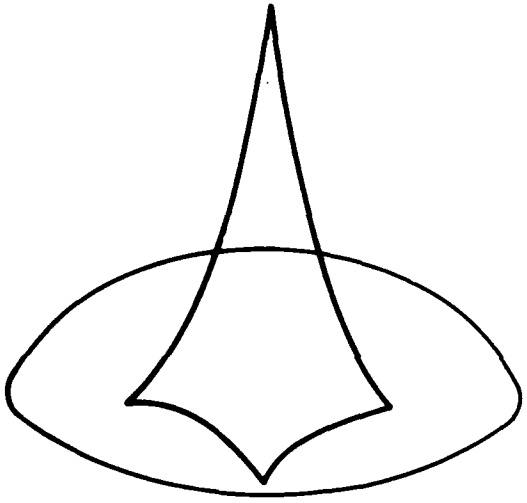

3 (a)

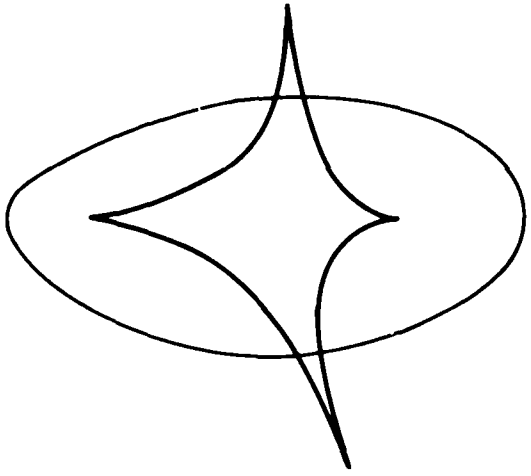

3 (b)

FIG. 3

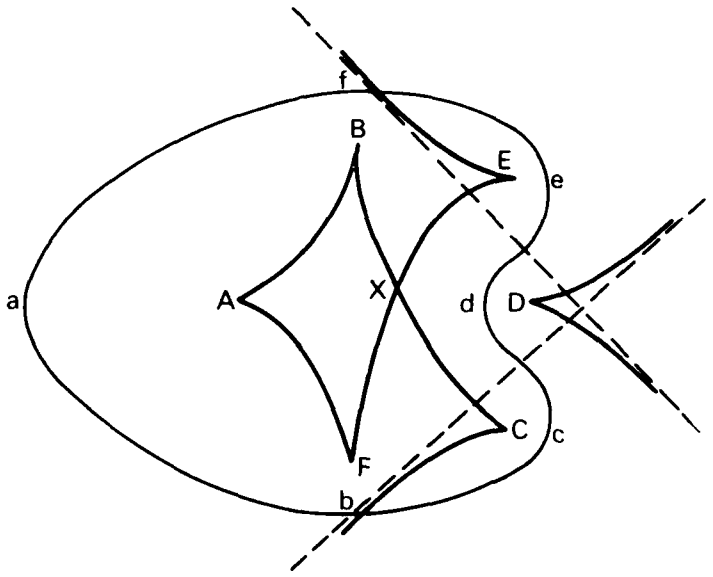

FIG. 4

DISTRIBUTION

AUSTRALIA

	Copy No.
Department of Defence	
Central Office	
Chief Defence Scientist	1
Deputy Chief Defence Scientist	2
Superintendent, Science and Technology Programs	3
Defence Library	4
Joint Intelligence Organisation	5
Assistant Secretary, DISB	6–21
Australian Defence Scientific and Technical Representative (U.K.)	22
Counsellor, Defence Science (USA)	23
Aeronautical Research Laboratories	
Chief Superintendent	24
Superintendent, Materials Division	25
Divisional File, Materials Division	26
Author: P. A. Doyle	27
Library	28
Materials Research Laboratories	
Library	29
Defence Research Centre, Salisbury	
Library	30
Central Studies Establishment	
Information Centre	31
Engineering Development Establishment	
Library	32
RAN Research Laboratory	
Library	33
Navy Office	
Naval Scientific Adviser	34
Army Office	
Army Scientific Adviser	35
Air Force Office	
Air Force Scientific Adviser	36
Aircraft Research and Development Unit	37
Technical Division Library	38
Department of Productivity	
Government Aircraft Factories	
Library	39

Department of Transport

Secretary		40
Library		41

Statutory, State Authorities and Industry

Australian Atomic Energy Commission, Director		42
CSIRO Mechanical Engineering Division, Chief		43
CSIRO National Measurement Laboratory, Chief		44
CSIRO Materials Science, Director		45
Gas & Fuel Corporation of Victoria, Research Director		46
SEC Herman Research Laboratory, Librarian, Victoria		47
SEC of Queensland, Library		48
BHP Central Research Laboratories, NSW		49
BHP Melbourne Research Laboratories		50

Universities and Colleges

Adelaide	Barr Smith Library	51
Flinders	Library	52
James Cook	Library	53
Latrobe	Library	54
Melbourne	Engineering Library	55
Monash	Library	56
	Professor I. J. Polmear, Materials Engineering	57
Newcastle	Library	58
New England	Library	69
New South Wales	Physical Sciences Library	60
Queensland	Library	61
	Professor A. F. Pillow, Applied Mathematics	62
Sydney	Professor R. Wilson, Applied Mathematics	63
Tasmania	Engineering Library	64
Western Australia	Library	65
	Dr P. B. Chapman, Mathematics	66
RMIT	Library	67

CANADA

Physics and Metallurgy Research Laboratories, Dr A. Williams	68
NRC, National Aeronautical Establishment, Library	69

Universities

McGill	Library	70

FRANCE

AGARD, Library	71
Gaz de France, Library	72
Institut Francais de Petrole, Library	73
ONERA, Library	74
Service de Documentation Technique de l'Aeronautique	75

GERMANY

ZLDI	76

INDIA

CAARC Co-ordinator Materials	77
Indian Institute of Science, Library	78
Indian Institute of Technology, Library	79
National Aeronautical Laboratory (Director)	80

International Committee on Aeronautical Fatigue
(Through Australian ICAF Representative) 81–107

END

DATE
FILMED

8-80

DTIC